Structural and Functional Classes of Multipolar Cells in the Ventral Cochlear Nucleus

JOHN R. DOUCET[1]* AND DAVID K. RYUGO[1,2]
[1]Department of Otolaryngology-Head and Neck Surgery, Johns Hopkins University School of Medicine, Baltimore, Maryland [2]Department of Neuroscience, Johns Hopkins University School of Medicine, Baltimore, Maryland

ABSTRACT

Multipolar cells in the ventral cochlear nucleus (VCN) are a structurally and functionally diverse group of projection neurons. Understanding their role in the ascending pathway involves partitioning multipolar cells into distinct populations and determining where in the brain each sends its coded messages. In this study, we used retrograde labeling techniques in rats to identify multipolar neurons that project their axons to the ipsilateral dorsal cochlear nucleus (DCN), the contralateral CN, or both structures. Three rats received injections of biotinylated dextran amine in the ipsilateral DCN and diamidino yellow in the contralateral CN. Several radiate multipolar neurons (defined by their axonal projections to the ipsilateral DCN and their dendrites that traverse VCN isofrequency sheets) were double-labeled but over 70% were not. This result suggests two distinct populations: (1) radiate-commissural (RC) multipolar cells that project to the ipsilateral DCN and the contralateral CN, and (2) radiate multipolar cells that project exclusively (in this context) to the ipsilateral DCN. In a different group of animals, we retrogradely labeled multipolar neurons that project their axons to the contralateral CN and measured the size of their cell bodies. The mean size of this population ($266 \pm 156\ \mu m^2$) was significantly smaller than those of RC-multipolar cells ($418 \pm 140\ \mu m^2$). We conclude that the CN commissural pathway is composed of at least two components: (1) RC multipolar cells and (2) commissural multipolar cells that are small- and medium-sized neurons that project exclusively (in this context) to the contralateral CN. These results identify separate structural groups of multipolar cells that may correspond to physiological unit types described in the literature. They also provide protocols for isolating and studying different populations of multipolar cells to determine the neural mechanisms that govern their responses to sound. Anat Rec Part 288A:331–344, 2006.

Key words: hearing; ascending pathways; classifying neurons; naming neurons

Information about sound is conveyed to the brain by patterns of action potentials in the auditory nerve. These patterns are analyzed first by neurons in the cochlear nucleus (CN) that are the source of all ascending pathways in the central auditory system. An important step toward understanding the neural circuits that underlie hearing is to define how CN neurons divide, select, and encode the enormous amount of acoustic information that they receive.

Dendritic morphology can be used to partition ventral cochlear nucleus (VCN) projection neurons into three groups: bushy, multipolar, and octopus. Octopus cells are located in the caudal pole of the VCN and they are distinguished by several long dendrites that extend from one side of the cell body. Bushy cells usually have one or two primary dendrites. Shortly after arising from the soma, each primary dendrite ends in a spray of thinner and

Grant sponsor: National Institute on Deafness and Other Communication Disorders; Grant number: R01 DC006268, R01 DC04395, and P30 DC05211.

*Correspondence to: John R. Doucet, Johns Hopkins University, SOM, 720 Rutland Avenue, 420 Ross, Baltimore, MD 21205. Fax: 410-614-4748. E-mail: johnrdoucet@yahoo.com

Received 29 December 2005; Accepted 29 December 2005
DOI 10.1002/ar.a.20294
Published online 20 March 2005 in Wiley InterScience (www.interscience.wiley.com).

shorter dendrites. This study is concerned with multipolar cells. The dendrites of multipolar neurons branch much less frequently than those of bushy cells. Multipolar cells vary with respect to the number, length, thickness, orientation, and amount of dendritic branching. It is difficult to capture this heterogeneity with one name. "Multipolar" originally was used to describe neurons stained with cresyl violet whose multiple dendrites gave the cell body a polygonal (or multipolar) shape (Osen, 1969). In this study, multipolar cells refer to stellate, giant, and other types of nonbushy and nonoctopus cells defined using dendritic morphology (Brawer et al., 1974). We use the term "multipolar" to encompass the multipolar, giant, and small cells defined using somatic morphology (Osen, 1969).

Multipolar cells generate at least half of the efferent axons of the VCN (Osen, 1970). Like bushy cells, they project to several nuclei in the lower brain stem (Cant and Benson, 2003). Unlike the axons of bushy and octopus cells, those of multipolar neurons collateralize extensively within the CN (Smith and Rhode, 1989; Oertel et al., 1990; Palmer et al., 2003). They are the only VCN neurons that make direct projections to the inferior colliculus (Adams, 1979, 1983) and the contralateral CN (Cant and Gaston, 1982; Schofield and Cant, 1996a). The large number of multipolar neurons and direct projections to the midbrain imply that they are important components of the ascending pathway.

Some of the earliest descriptions of the CN recognized that multipolar cells were comprised of functionally distinct classes (Harrison and Irving, 1965, 1966; Osen, 1969; Lorente de Nó, 1981). In any region of the brain, partitioning the resident neurons into distinct classes is important for at least two reasons (Josephson and Morest, 1998; Carcieri et al., 2003). First, models of auditory processing in the brain stem are based on different CN cell types organized into neural circuits. Valid models depend on accurate identification of these cell types, their respective responses to sound, and their axonal connections. Second, information about each cell type serves as a baseline to interpret changes induced by deafness or noise-induced damage in terms of their effect on neural codes. Such information can then guide the development of intervention strategies such as prostheses.

Four questions drive our study of VCN multipolar neurons. What patterns of activity are recorded from multipolar cells in response to sound? What structural features determine why one multipolar neuron responds differently than another? What message does each type of response convey to the rest of the brain? Where in the brain are these different messages sent? Most tools allow only one or two of these questions to be addressed at a given time. Ultimately, the answers need to be synthesized within different populations of cells to determine their respective roles in the auditory pathway. In this article, we will illustrate a step toward such a synthesis by applying differences in axonal projection patterns to identify new structural classes of multipolar cells.

Structural Classes of VCN Multipolar Cells

Figure 1 displays features of two well-defined classes of multipolar cells and the three names for each class that are used in the literature. The names are based on differences between the groups with respect to somatic innervation, axonal trajectory, and dendritic morphology. First, ultrastructural profiles observed with the electron microscope resulted in the division of VCN multipolar cells in cats (Cant, 1981). Type I multipolar neurons receive very few synaptic contacts on their cell body, whereas Type II somata are covered with synaptic endings (Fig. 1A). Second, the parent axons of multipolar cells follow different paths in the CN. Most can be traced into the trapezoid body (or ventral acoustic stria) and were named T-stellate neurons in mice (Oertel et al., 1990). In contrast, the parent axons of D-stellate neurons project dorsally beneath the dorsal cochlear nucleus (DCN; Fig. 1B). Most of our knowledge pertaining to the neural mechanisms that govern the responses of multipolar neurons derives from in vitro descriptions of T- and D-stellate cells. T- and D-stellate neurons differ with respect to their intrinsic electrical properties (Oertel et al., 1990; Ferragamo et al., 1998; Fujino and Oertel, 2001). Both receive input from the auditory nerve (AN), but different sources of non-AN input target T- vs. D-stellate cells (Fujino and Oertel, 2001). For example, D-stellate cells inhibit T-stellate neurons (Ferragamo et al., 1998). The third set of commonly encountered names for the two classes is based on dendritic morphology as characterized in rats (Doucet and Ryugo, 1997). The dendrites of planar multipolar cells are oriented parallel to the path of auditory nerve fibers as they enter the CN (Fig. 1C). Consequently, their dendrites are confined to a plane formed by a small group of fibers that respond best to a narrow range of frequencies (i.e., a CN isofrequency plane). The dendrites of radiate multipolar cells project far from the soma and traverse isofrequency planes. Additional types of multipolar cells have been proposed but they have not been studied systematically (Brawer et al., 1974; Doucet and Ryugo, 1997).

Correlations between the features illustrated in Figure 1 indicate two definable classes of multipolar cells (Cant, 1981; Cant and Gaston, 1982; Smith and Rhode, 1989; Oertel et al., 1990; Doucet and Ryugo, 1997; Josephson and Morest, 1998; Friedland et al., 2003). For now, it seems the names "Type I," "T-stellate," and "planar" identify one group of cells and "Type II," "D-stellate," and "radiate" refer to the second group. Hereafter, we will use the terms "planar" and "radiate" for simplicity and because we will present new data generated from rats.

Planar and radiate multipolar cells differ in other ways. Radiate multipolar cells are glycinergic (Wenthold, 1987; Alibardi, 1998; Doucet et al., 1999b). The neurotransmitter used by planar multipolar cells is not known but different types of evidence suggest that they are excitatory (Smith and Rhode, 1989; Zhang and Oertel, 1993; Ferragamo et al., 1998). Radiate multipolar neurons project their axons to the contralateral CN but not to the contralateral inferior colliculus (IC; Fig. 1D). Planar multipolar cells project to the contralateral IC but not to the contralateral CN. These differences in morphology, inputs, cellular mechanisms, neurochemistry, and axonal projections indicate that planar and radiate multipolar cells almost certainly have different functions in the auditory system.

Physiological Units Recorded From VCN Multipolar Cells

Table 1 summarizes the responses to sound recorded from VCN multipolar cells. Recordings were verified to be from multipolar cells in one of two ways: (1) directly by intracellularly labeling the neuron at the end of the re-

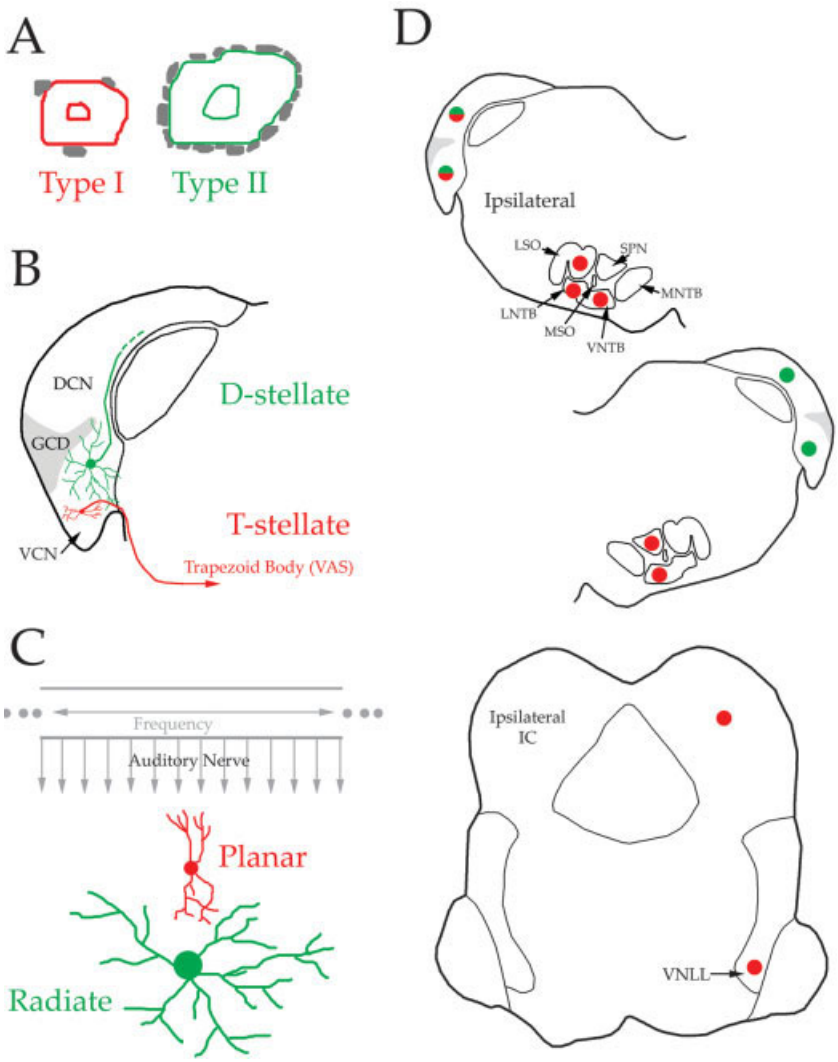

Fig. 1. Morphological features that distinguish two types of VCN multipolar cells. Red and green are used to link characteristics associated with each class. **A–C** display features that underlie the different names for these two classes frequently encountered in the literature. A: Ultrastructural profiles of the cell body with gray areas denoting synaptic terminals (Cant, 1981). B: Trajectory of the parent axon in the CN (Oertel et al., 1990). The dendrites of D-stellate neurons frequently end in the granule cell domain. C: Dendritic orientation with respect to the array of auditory nerve fibers (Doucet and Ryugo, 1997). Structures in gray depict the cochlear frequency axis and auditory nerve fibers. Planar multipolar cells receive input from fibers derived from a narrow region of the cochlea, whereas radiate multipolar cells are innervated by fibers spread over a broad region of the cochlea. **D:** Axonal targets of VCN multipolar cells residing in the left CN. Red dots denote input from planar multipolar cells; green dots, input from radiate multipolar cells; green and red dots, input from both classes. This summary of targets derives from a recent review (Cant and Benson, 2003) except that minor targets (e.g., ipsilateral IC) are not shown. DCN, dorsal cochlear nucleus; GCD, granule cell domain; IC, inferior colliculus; LSO, lateral superior olive; LNTB, lateral nucleus of the trapezoid body; MNTB, medial nucleus of the trapezoid body; MSO, medial superior olive; SPN, superior paraolivary nucleus; VCN, ventral cochlear nucleus; VNLL, ventral nucleus of the lateral lemniscus; VNTB, ventral nucleus of the trapezoid body.

cording, or (2) indirectly via antidromic activity that was elicited by electrical shocks to the contralateral IC or contralateral CN. An intracellular labeling study that was not included in Table 1 (Friauf and Ostwald, 1988) filled several VCN neurons in rat that they referred to as multipolar/stellate cells. However, the axons of these neurons formed endbulb-like terminals in the ventral nucleus of the lateral lemniscus, a signature of octopus cells (Vater and Feng, 1990; Schofield, 1995; Adams, 1997). Physiological units usually are classified by the shape of their poststimulus time (PST) histogram in response to a brief tone (Pfeiffer, 1966). In Table 1, 105 of 110 units recorded from multipolar cells responded as chopper or onset units. The PST histograms of chopper units have several distinct peaks because they fire at regular time intervals during the tone. Onset units have a very large peak shortly after tone onset, indicating that the first action potential fired by these units tends to occur at the same time relative to tone onset (and thus collect in a single time bin). The steady-state firing rates of onset units are lower than other unit types, but those recorded from identified multipolar cells fire more than one action

TABLE 1. Physiological unit types recorded from different classes of VCN multipolar neurons

		Planar multipolar neurons							Radiate multipolar neurons							Unclassified multipolar neurons						
		chopper units			onset units			Other	chopper units			onset units			Other	chopper units			onset units			Other units
	Species	S	T	O	C	L	O	units	S	T	O	C	L	O	units	S	T	O	C	L	O	
Bourk, 1976	cat	7	9	5			4	2														
Rhode, Oertel, Smith 1983	cat	2	3										1					9				
Rouiller and Ryugo, 1984	cat																1					
Smith and Rhode, 1989	cat	5										4										
Ostapoff, Feng, Morest 1994	gerbil, chinchilla	1														5						3
Paolini and Clark 1999	rat											7										
Palmer, Wallace, Arnott, Shackleton 2003	guinea pig	7	6	2								5	3									
Needham and Paolini 2003	rat											7										
Smith, Massie, Joris 2005	cat											7	1									
Totals		22	18	7	0	0	4	2	0	0	0	30	5	0	0	5	1	9	0	0	0	3

C, onset chopper; L, onset-low sustained rate; O, other or unclassified types of chopper or onset unit; S, sustained chopper; T, transient chopper.

potential in response to a tone. Onset units that fire only one action potential (onset-inhibitory or OnI units) are rare and probably are recorded from octopus cells (Godfrey et al., 1975; Rhode et al., 1983; Rouiller and Ryugo, 1984; Smith et al., 2005).

We used the morphological descriptions of the authors to classify each physiological unit in Table 1 as a planar or radiate multipolar cell. All of the features in Figure 1 were employed but most units were classified by whether their parent axon projected dorsally or ventrally. Units were placed in the "unclassified multipolar neuron" category for two reasons: (1) the description of morphology was sparse or, rarely, (2) the unit had features associated with both planar and radiate multipolar cells [e.g., the axon projected into the trapezoid body (planar) but had dendrites that ended in the granule cell domain (radiate)]. Physiological units that could be activated antidromically with shocks to the IC (Bourk, 1976) were classified as planar multipolar cells (Cant, 1982; Schofield and Cant, 1996b; Josephson and Morest, 1998). Units driven by shocks to the contralateral CN (Needham and Paolini, 2003) were classified as radiate multipolar cells (Wenthold, 1987; Schofield and Cant, 1996a, 1996b; Doucet et al., 1999b). The studies listed in Table 1 demonstrate that most planar multipolar cells respond to tones as chopper units (47 out of 53), whereas radiate multipolar neurons are onset units.

Chopper and onset units have been divided into several subclasses. There are at least two types of chopper units (Bourk, 1976; Young et al., 1988): transient (ChT) and sustained (ChS). Onset units have been partitioned into onset chopper (OnC) units that fire regularly near tone onset and others that have low sustained firing rates (OnL) (Godfrey et al., 1975; Rhode and Smith, 1986; Winter and Palmer, 1995). A few points are germane to this discussion. First, roughly equal proportions of ChT and ChS units are encountered in surveys of VCN neurons (Bourk, 1976; Blackburn and Sachs, 1989). The same is true for OnC vs. OnL units (Godfrey et al., 1975; Winter and Palmer, 1995). Second, the subclasses of chopper and onset units differ with respect to first-spike latency, dynamic range, tuning, and presence of inhibitory side bands (Rhode and Smith, 1986; Kim et al., 1991; Rhode and Greenberg, 1994). These data suggest that the four unit types are recorded from distinct populations of multipolar cells. Third, different types of chopper and onset units are recorded from the same structural class (Table 1). Some features of dendrites and/or axons appear to correlate with the various units (Rhode et al., 1983; Palmer et al., 2003; Arnott et al., 2004), but our understanding of the structural basis for the physiological diversity of multipolar cells is incomplete.

Are There Subclasses of Planar and Radiate Multipolar Cells?

What structural features cause one radiate multipolar neuron to respond as an OnC unit and another to respond as an OnL unit? Do these two unit types reflect biological variability in the structure of radiate multipolar cells or is this group actually comprised of two distinct structural

classes that correspond to the two unit types? The direct approach is to define the structure of neurons within each unit class using in vivo intracellular recording and filling of single cells. However, this method is very difficult. Another approach is to label large populations of multipolar cells, quantify various aspects of their morphology (e.g., dendritic field), and use statistical criteria to delineate separate groups. This approach has been used successfully to define classes of amacrine, bipolar, and ganglion cells in the retina (Dacey et al., 2003; Badea and Nathans, 2004; Connaughton et al., 2004). Fortunately, unlike inner retinal neurons, VCN multipolar cells project their axons far outside the CN. Functional distinctions between populations of neurons should correlate with differences in axonal projection patterns, providing a means (with retrograde labeling techniques) to isolate and define different types of multipolar cells. For example, planar (chopper units) and radiate (onset units) multipolar cells are hypothesized to encode different aspects of sounds and these codes are distributed to different parts of the brain (Fig. 1D). Similarly, if OnC and OnL units subserve different roles, there should be two corresponding types of radiate cells that differ with respect to their axonal connections. Indeed, in one study, five intracellularly filled OnC units projected their axons to the contralateral CN but three labeled OnL units did not (Arnott et al., 2004). In this study, we tested the hypothesis that multipolar cells with radiate-like morphology were comprised of two distinct populations by examining their projections to the ipsilateral DCN and the contralateral CN.

MATERIALS AND METHODS

Data were obtained from seven male Sprague-Dawley rats weighing between 320 and 390 g. All animals were used in accordance with the National Institutes of Health guidelines and the approval of the Animal Care and Use Committee for the Johns Hopkins University School of Medicine.

Tissue sections were viewed and analyzed with a Nikon E600 microscope equipped for brightfield and epifluorescence microscopy. Digital photographs were collected with a CCD color camera (Hamamatsu C5810). Brightness or contrast was modified (if necessary) using Adobe Photoshop.

Experiment 1

Tracer injection and tissue processing. Four rats were used to define the size and distribution of VCN multipolar cells that project their axons to the contralateral CN. In two animals, the left CN was injected with Fast Blue (FB; 3% solution in distilled water; Polysciences, Warrington, PA). The other two animals received an injection of Fluorogold (FG; 3% solution in distilled water; Biotium, Hayward, CA). Surgical procedures for exposing the CN followed those described previously (Doucet and Ryugo, 1997). Rats were anesthetized with an intraperitoneal injection of sodium pentobarbital (45 mg/kg) and then given an intramuscular injection of atropine sulfate (0.05 mg). When the animal was areflexic to a paw pinch, the CN was exposed and a glass pipette (inner diameter of tip: 30–50 μm) filled with tracer was advanced toward the nucleus. Pressure was applied with a nanoliter injector (Drummond, Broomall, PA) and 20–50 nl of tracer was injected at several depths and locations (Fig. 2A).

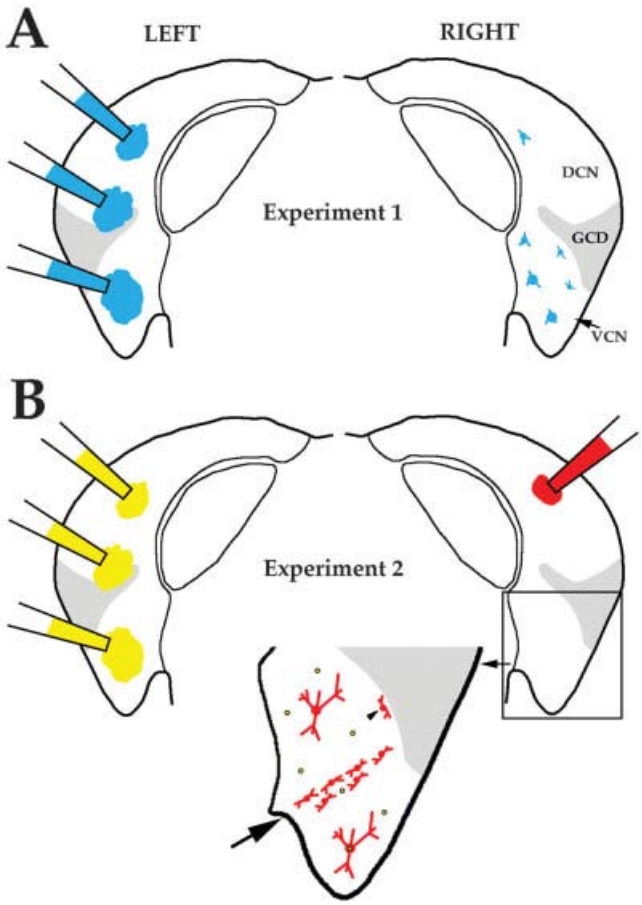

Fig. 2. Illustration of protocols and expected labeling patterns for the experiments performed in this study. **A** and **B** each display coronal sections through the left and right CN. A: In experiment 1, FG or FB (depicted) was injected at several locations within the left CN to label VCN multipolar cells retrogradely in the right CN. Both tracers fill the soma (and proximal dendrites) of labeled VCN neurons, allowing us to characterize the size and location of their cell bodies. A few cells were labeled in the DCN but these were not analyzed. B: In experiment 2, DiY was injected at several locations within the left CN to label VCN multipolar cells retrogradely in the right VCN. DiY primarily labels the nucleus and labeled nuclei in the right VCN are depicted as yellow dots surrounded by black circles. In the same animal, a small injection of BDA was made in the right DCN. BDA is colored red because it was visualized with Cy3. BDA fills the soma and frequently the dendritic tree of labeled cells. Small BDA injections in the DCN produce a stripe of labeled planar multipolar cells in the corresponding frequency region of the ipsilateral VCN (large arrow). Labeled marginal multipolar cells (arrowhead) are observed adjacent to the granule cell domain. Two labeled radiate multipolar cells are shown, identified in this illustration by their large size and location outside the stripe of planar multipolar cells. Our hypothesis is that some radiate multipolar cells will also contain DiY (double-labeled cell below stripe), whereas others will only contain BDA (single-labeled cell above stripe). The number of double- vs. single-labeled radiate multipolar cells provides information about whether all radiate multipolar cells project to both the ipsilateral DCN and the contralateral CN. By comparing the size distribution of double-labeled radiate multipolar cells in experiment 2 with the size distribution of labeled multipolar cells in experiment 1, we can test whether radiate multipolar cells are the sole source of the CN commissural pathway.

After allowing the animals to recover and survive for 6 days, they were deeply anesthetized with a lethal dose of sodium pentobarbital (100 mg/kg) and perfused through the heart with fixative [4% paraformaldehyde in 0.1 M phosphate buffer (PB), pH 7.4]. The brain was dissected, blocked, cryoprotected, and sectioned (40 μm) in the coronal plane. After FB injections, all sections were mounted on subbed slides, allowed to air-dry, and coverslipped with Krystalon. For FG injections, labeled cells were visualized with an immunohistochemical protocol. All procedures were performed on a shaker table at 4°C and the sections were washed with phosphate-buffered saline (PBS; 0.05 M; pH 7.4) between each step. First, the sections were placed in a blocking solution [0.2% Triton X-100, 5% normal goat serum (Chemicon, Temecula, CA) made in PBS] for 1 hr. Then, they were incubated for 72 hr in rabbit anti-FG (Chemicon) that was diluted 1:20,000 in the blocking solution. Staining caused by endogenous peroxidase was reduced by placing the sections in a 0.3% solution of hydrogen peroxide (in PBS). This step was followed by a 90-min incubation in biotinylated goat anti-rabbit (Jackson Immunoresearch Laboratories, West Grove, PA) that was diluted 1:1,000 in the blocking solution. Finally, the sections were processed using a standard NiDAB protocol, mounted on slides, dehydrated, cleared in xylene, and coverslipped with Permount.

Data collection and analysis. The injection site was documented by photographing at least every other section through the nucleus with a 10× objective (NA = 0.5). Camera parameters were set by first photographing a section through the center of the injection site. These same camera parameters remained constant for all the remaining sections. In each tissue section, several photographs were necessary to capture the CN and they were stitched together in Photoshop. The region filled with FB, FG, or Diamidino Yellow (DiY) was summarized by partitioning the injection site into two regions: a core and a halo. The core represents a very bright area (or dark area for FG injections after DAB processing) that contains a high concentration of tracer. The axons of labeled cells in the contralateral CN probably form synaptic terminals in the core or pass through this region. They may also pass through the halo that was less bright (dark) and contained a lower concentration of tracer.

To analyze FG- or FB-labeled cells in the contralateral CN, a low-magnification photomontage (10× objective) was constructed of every other section through the contralateral CN. We then returned to these sections and photographed each labeled cell at high magnification (40×, NA = 0.95). The position of each cell was noted on the low-magnification maps so that soma size could be correlated with location. The silhouette of the cell body was traced in Photoshop and area measurements were obtained with a commercially available plugin (Reindeer Graphics, Asheville, NC). These data are presented as mean ± standard deviation.

Experiment 2

Tracer injection and tissue processing. Three rats were used to describe the size and distribution of VCN multipolar cells that project to the ipsilateral DCN and/or the contralateral CN. Surgical procedures for exposing the two cochlear nuclei were identical to those described above. Figure 2B illustrates the injection protocol. We made a large injection of DiY (3% solution in distilled water; Sigma, St. Louis, MO) in the left CN. In the right CN, a glass pipette (inner diameter of tip, 10–15 μm) containing biotinylated dextran amine (BDA; 10,000 MW; 10% solution in 0.01 M PB; Invitrogen-Molecular Probes, Carlsbad, CA) was advanced 200–300 μm below the surface of the DCN. BDA was ejected using positive current pulses (5 μA; 7 sec on/7 sec off) applied for 5 min. After allowing the animals to survive between 4 and 9 days, their brains were fixed and sectioned as described above. Sections through the CN were incubated overnight in PBS containing streptavidin conjugated to Cy3 (1:10,000; Jackson Immunoresearch Labs). All sections were mounted on subbed slides, allowed to air-dry, and coverslipped with Krystalon. At this point, the soma and dendrites of BDA-labeled cells fluoresce red and the nucleus of DiY-labeled cells fluoresces yellow.

Data collection and analysis. The procedure for documenting the DiY and BDA injection sites was identical to the one described above for the FB and FG injections. In the VCN ipsilateral to the DCN injection site, DiY- and BDA-labeling were viewed using different epifluorescence filter sets. Low-magnification (10×) maps of each type of labeling were obtained by photographing every other section through the right CN with one filter set and then the other. The two maps were aligned in Photoshop using landmarks such as the borders of the nucleus and blood vessels. We then returned to these sections and examined every DiY-labeled cell (40× objective). The microscope was focused on the DiY-labeled nucleus and switched to the other filter set to determine if the neuron also contained BDA-Cy3 labeling. We classified the cell as double-labeled when the DiY-labeled nucleus was clearly within the borders of the BDA-Cy3-labeled cytoplasm and both tracers were present in the same focal plane. The sizes of BDA-labeled neurons were measured as described above.

RESULTS

Identifying and Naming Multipolar Cells

Identifying and discussing neuronal classes is influenced by the names we give them (Rowe and Stone, 1977). Names for cell populations have a historical context but as new data emerge their definitions tend to change. Our goal is to identify and name VCN multipolar cells according to their axonal targets while referencing and respecting organizational schemes that already exist. In this study, for example, we identify populations of VCN multipolar cells in the context of their projections to the ipsilateral DCN and the contralateral CN. VCN multipolar neurons that project to the contralateral CN are referred to as VCN commissural cells (Schofield and Cant, 1996a; Alibardi, 1998). The morphology and neurochemistry of many VCN commissural neurons bear a striking resemblance to those of radiate multipolar cells that project to the ipsilateral DCN (Schofield and Cant, 1996a; Doucet and Ryugo, 1997). This resemblance led to the general notion that radiate multipolar neurons project to both structures, an idea supported by intracellularly filled radiate multipolar cells that send a collateral axon to the ipsilateral DCN before innervating the contralateral CN (Arnott et al., 2004; Smith et al., 2005). These results indicate that some radiate multipolar cells project to both structures, but they leave open the possibility that a dif-

ferent group of radiate multipolar cells projects exclusively (in this context) to the ipsilateral DCN. Indeed, this distinction is one of the results described in this study. How do we name these two different groups of radiate multipolar cells? We have chosen to reserve the name "radiate multipolar" for those neurons with radiate morphology that project exclusively to the ipsilateral DCN. Similarly, the term "commissural multipolar" will be used for neurons that project their axons exclusively to the contralateral CN. VCN multipolar neurons that have radiate-like morphology and that project to both structures will be referred to as radiate-commissural RC-multipolar cells. The utility of this approach to classifying and naming multipolar neurons is a working hypothesis that remains to be tested.

Figure 2 summarizes the protocols and goals for the two experiments performed in this study. In experiment 1 (Fig. 2A), we made large injections of FG or FB in one CN to label multipolar cells retrogradely in the opposite CN. This experiment allowed us to define the location and size of VCN multipolar cells that projected their axons to the contralateral CN. In experiment 2 (Fig. 2B), we made a large injection of DiY in one CN and a small injection of BDA in the contralateral DCN. The VCN ipsilateral to the injected DCN revealed three types of labeling: (1) multipolar cells that contained only BDA (red cytoplasm due to Cy3) projected to the ipsilateral DCN. The size of BDA-labeled cells can be measured because BDA filled the cytoplasm. (2) multipolar cells that contained both BDA and DiY (i.e., a red cytoplasm and a yellow nucleus) projected to both structures. These double-labeled cells were important because their size can be compared to the size of multipolar cells labeled in experiment 1. Similar size distributions for these two populations would suggest that all multipolar cells that project to the contralateral CN also send a collateral to the ipsilateral DCN. Dissimilar size distributions would imply that some multipolar cells that project to the contralateral CN do not send a collateral to the ipsilateral DCN. (3) multipolar cells that contained only DiY projected to the contralateral CN. We cannot measure the size of these neurons because DiY labels the nucleus.

Experiment 1: Multipolar Cells That Project to Contralateral CN

Figure 3A displays an FB injection in the left CN. Two features of this injection site were typical. First, the injection site was very large. Posterior regions of the nucleus were almost completely filled with tracer in each case but little or no tracer was deposited anterior to the entrance of the auditory nerve root. Second, the tracer spilled outside the borders of the CN (e.g., inferior cerebellar peduncle). Tracer in these areas, however, should not contaminate our results because cells in the right CN project through or near these regions only if they are innervating the left CN. We confirmed this assumption with an FB injection that was confined to the left CN. Fewer cells were labeled in the right CN of this case, but the size and distribution of the labeled cells were similar to those that received large injections.

Figure 3B displays commissural cells in one section through the right anteroventral CN (AVCN). Labeled cells were sparsely scattered throughout the nucleus. The dendrites of many were analyzed and defined as belonging to multipolar cells. As in cats (Cant and Gaston, 1982) and guinea pigs (Shore et al., 1992; Schofield and Cant, 1996a), the number of such neurons in rats is small. For the cases that received large injections, the total number of labeled cells in the right CN ranged from 244 to 506 (mean = 401 ± 111). Labeled neurons in the VCN outnumbered those in the DCN by nearly a factor of 10.

In guinea pigs, the size of commissural cells is highly variable (Shore et al., 1992; Schofield and Cant, 1996b). This description is also true for rats (Fig. 3C and D). Consider that over 90% of spherical bushy cells in the anterior pole of the rat VCN have somatic areas between 100 and 300 μm^2 (data not shown). If spherical bushy cells are defined as medium-sized VCN neurons, then many cells labeled in the two experiments summarized in Figure 3C and D are large or even giant multipolar cells (Cant and Gaston, 1982). In rats that had at least 350 labeled neurons in the right VCN, the percentage that had somatic areas greater than 300 μm^2 was 37%, 29%, and 26%. The corollary is that 60–75% of the labeled neurons had somatic areas less than 300 μm^2. This size distribution contrasts with that of radiate multipolar cells labeled by injecting BDA into the ipsilateral DCN (Doucet et al., 1999b), where we observed that only 10% of radiate multipolar neurons have somatic areas less than 300 μm^2. This size difference suggests that the source of the commissural pathway is comprised of at least two populations of multipolar cells. In the next section, we describe results from a different set of experiments designed to identify neurons that project to both the ipsilateral DCN and the contralateral CN.

Experiment 2: Multipolar Cells That Project to Ipsilateral DCN and/or Contralateral CN

The pattern of VCN labeling produced by a small tracer injection in the DCN has been described previously (Doucet and Ryugo, 1997; Ostapoff et al., 1999). The majority of BDA-filled structures was confined to the corresponding frequency region of the VCN and formed a stripe in coronal sections (Fig. 4A). VCN multipolar cells that project to the DCN can be partitioned into three structural classes in rats (Doucet and Ryugo, 1997). Planar multipolar cells comprised the vast majority of the labeled cells in the stripe. Radiate multipolar cells were located inside and outside the stripe. Marginal multipolar cells had a similar distribution to radiate multipolar cells with respect to the stripe but they were distinguished by their smaller size and location along the borders of the granule cell domain.

The large injection of DiY in the contralateral CN labeled the nuclei of cells scattered among the BDA-filled radiate, planar, and marginal multipolar neurons (Fig. 4A). Across all the cases, 50 neurons contained both BDA and DiY. The size and location of double-labeled cells differed from that of marginal multipolar neurons. Most of the 693 BDA-labeled neurons in the stripe were planar multipolar cells, and double-labeled cells in the stripe were rare (25/693 or $< 4\%$). We concluded that planar and marginal multipolar cells did not project to the contralateral CN. In contrast, in each rat, we observed several radiate multipolar neurons outside the stripe that contained both tracers (Fig. 4B). The size distribution of double-labeled cells (Fig. 5) is similar to the one we have published previously for radiate multipolar neurons (Doucet et al., 1999b). The somata of 32 double-labeled cells were located in the stripe or within 100 μm above or

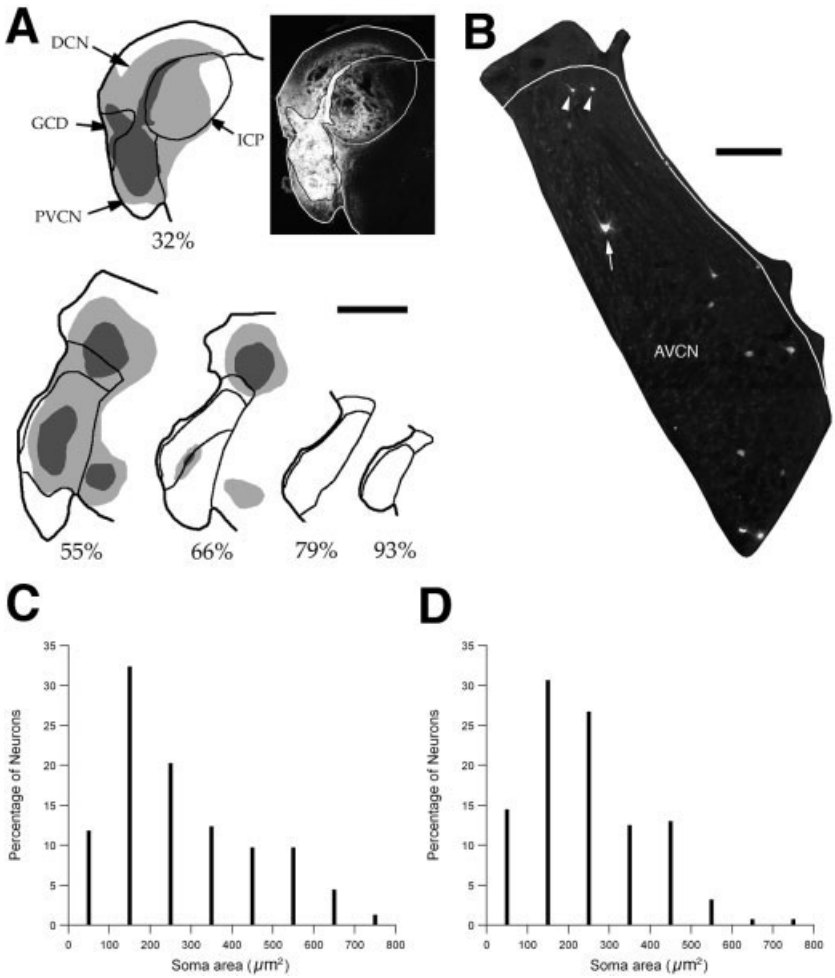

Fig. 3. Experiment 1: labeling of VCN multipolar cells that project to the contralateral CN. Data for **A–C** were taken from one rat that received an FB injection in the left CN. A: FB injection site in the CN. The location of each section through the CN along the anterior/posterior axis is expressed as a percentage of the total length of the CN (0% equals the posterior border of the DCN). The core portion of the injection site is shown as dark gray and the halo is light gray. These two regions are illustrated for one section through the DCN and PVCN in the photograph to the right of the drawing. Scale bar = 1 mm. B: Fluorescent micrograph of a section through the contralateral CN shows several FB-labeled cells. Large (arrow) and small (arrowhead) commissural multipolar cells were labeled. Border of GCD is drawn in white. Scale bar = 200 μm. C: Size histogram for FB-labeled cells (191 cells). **D:** Size histogram for VCN cells labeled in a different rat that received an injection of FG in the left CN (204 cells). The similar size distributions in the two panels indicate that they are independent of the tracer used to label these neurons. AN, auditory nerve; AVCN, anterior ventral cochlear nucleus; ICP, inferior cerebellar peduncle; PVCN, posterior ventral cochlear nucleus.

below the stripe. This pattern is consistent with the projections of radiate multipolar cells to the DCN because the soma (in the VCN) and the center of the broad terminal field (in the DCN) appear to be in corresponding frequency regions (Arnott et al., 2004; Smith et al., 2005). Since the double-labeled cells project their axons to the ipsilateral DCN and the contralateral CN, we will refer to this population as RC-multipolar cells.

In Figure 5, the size distribution of RC-multipolar cells is compared to that of multipolar cells labeled in experiment 1 with unilateral FB injections in the CN. The mean size of RC-multipolar cells (418 ± 140 μm^2) is significantly larger than that of the entire population of multipolar cells that project to the contralateral CN (266 ± 156 μm^2; $P < 0.0001$, Wilcoxon/Kruskal-Wallis test). Over 40% of the multipolar cells labeled in experiment 1 have somatic areas less than 200 μm^2, whereas less than 10% of RC-multipolar cells are this small. Collectively, these results suggest that a group of small- and medium-sized multipolar cells project their axons to the contralateral CN but do not send a collateral to the ipsilateral DCN. A corollary finding is that RC-multipolar neurons account for only a portion of the CN commissural pathway.

Are There Two Types of Multipolar Cells With Radiate Morphology?

We addressed this question with data obtained from experiment 2. Radiate (cells labeled only with BDA) and RC-multipolar (cells labeled with BDA and DiY) neurons were distinguished from marginal multipolar cells by their size and distribution within the VCN core (i.e., at least 50 μm from the border of the granule cell domain). They were separated from planar multipolar cells by their location at least 50 μm ventral to the stripe of BDA label-

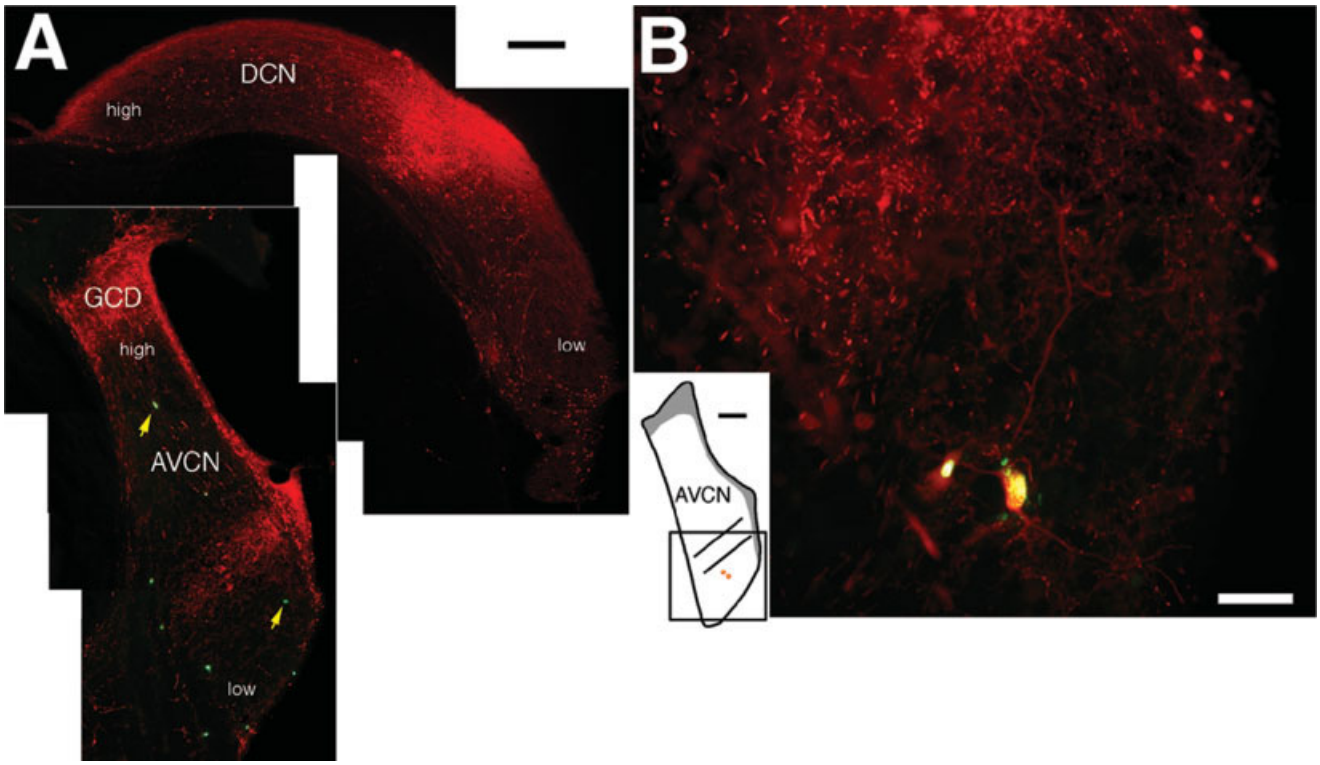

Fig. 4. Results from a rat that received a DiY injection in the left CN and a BDA injection in the right DCN. **A:** Fluorescent micrographs of two coronal sections display the BDA injection site (red) in the right DCN (top) and the pattern of labeling in the ipsilateral VCN. The location of VCN and DCN neurons that respond best to high or low frequencies is indicated. Injections that are confined to a narrow portion of the DCN frequency axis produce a stripe of BDA labeling in the corresponding frequency region of the VCN. Several DiY-labeled cells can also be seen scattered within the VCN and two are indicated by arrows. The photograph of the AVCN was produced by aligning photomontages of the two types of labeling and then combining the images. Scale bar = 200 μm. **B:** Fluorescent photomicrograph displaying two double-labeled cells. The location of both cells with respect to the stripe of BDA label is shown in the inset. Scale bar = 50 μm.

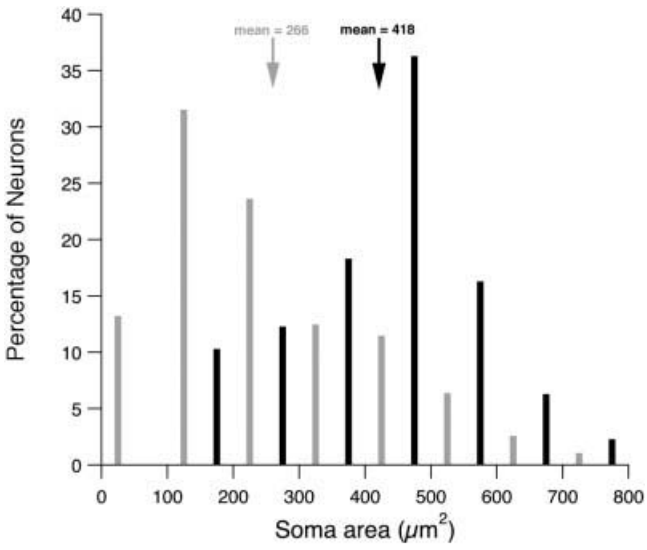

Fig. 5. Size histogram for RC-multipolar cells (black, 50 cells) and commissural multipolar neurons (gray, 386 cells). The commissural multipolar neurons were labeled in two rats that received injections of FB in the left CN.

ing (Fig. 6). Planar multipolar cells in this low frequency region of the VCN will not be labeled because they project to low-frequency regions of the DCN—lateral to the BDA injection site (Friedland et al., 2003). For each animal, there were at least 20 BDA-labeled cells and between 100 and 145 DiY-labeled cells in this ventral region of the VCN. Most of these BDA-labeled cells contained only BDA, even though their size and dendritic morphology clearly placed them in the radiate class (Fig. 6). For each case, the number of radiate multipolar cells outnumbered RC-multipolar cells by more than a factor of 3. The average size of radiate multipolar cells (379 μm^2) was similar to RC-multipolar cells (stated above). We also did not observe any difference in their dendritic morphology.

Such a low incidence of double labeling could be caused by incompatible tracers but this explanation is unlikely given that BDA collects in the cytoplasm and dendrites, whereas DiY primarily fills the nucleus. Also, in a different type of experiment, we injected BDA into the DCN and DiY into the contralateral IC. In this case, nearly 80% of planar multipolar cells were double-labeled (Doucet et al., 1999a), ruling out dye incompatibility. Another possibility is that the CN commissural pathway was incompletely filled, given that the DiY injection did not spread into the rostral AVCN. However, most of this pathway enters the CN via the dorsal and intermediate acoustic stria and the

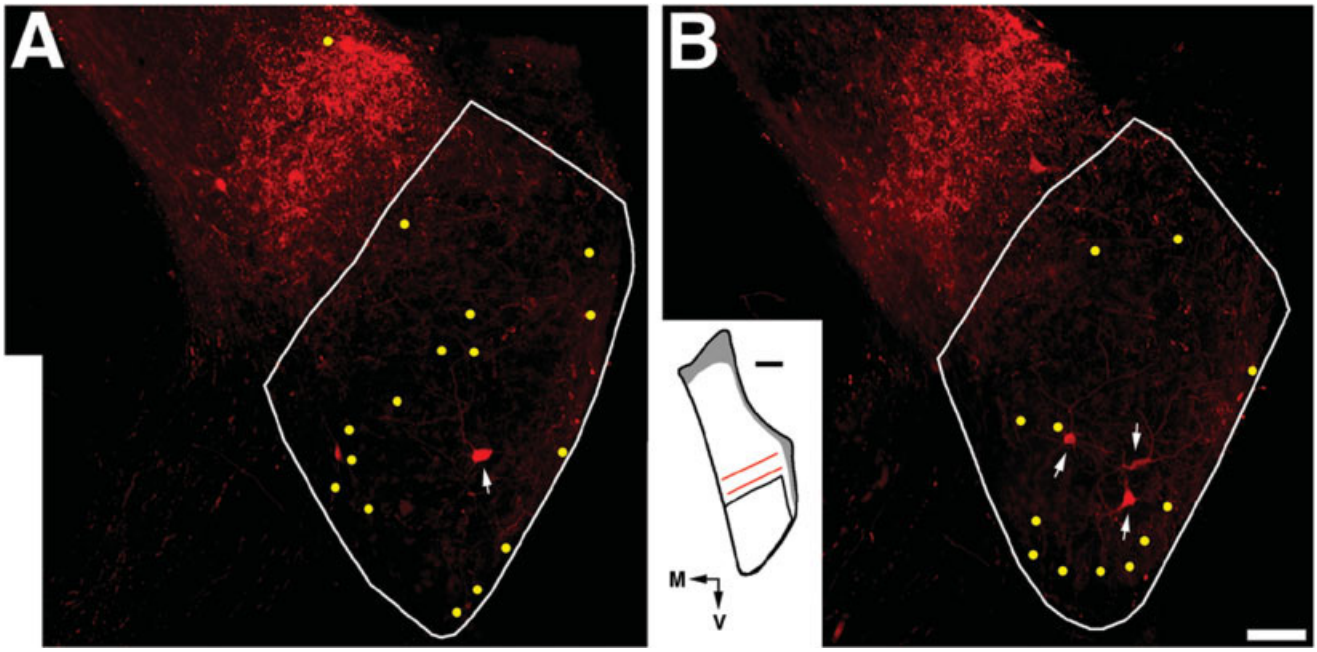

Fig. 6. **A** and **B:** Fluorescent micrographs of BDA and DiY labeling in two sections through the right AVCN. This rat was part of experiment 2 (Fig. 2). The two sections were separated by 80 microns. The inset is a drawing of the section in **B** that shows the borders of the granule cell domain (gray), the stripe of BDA labeling (red), and the borders of a region ventral to the stripe. The labeled cells in this ventral region were analyzed to determine if radiate multipolar cells (some denoted with arrows) differed with respect to their projections to the contralateral CN. The locations of DiY-labeled cells (yellow dots) within each section and an adjacent section are plotted. The majority of radiate multipolar cells only contained BDA. Scale bars = 200 μm (inset); 100 μm (micrograph). M, medial; V, ventral.

individual axons seem to innervate large areas of the DCN and/or VCN (Cant and Gaston, 1982; Shore et al., 1992). Thus, the DiY injection filled the area traversed by commissural axons (to facilitate labeling by axons of passage) and most likely overlapped with their terminal fields. Consistent with this view of the injection site, radiate multipolar cells labeled with BDA usually were surrounded by DiY-labeled cells (Fig. 6). Finally, more single-labeled cells of each kind did not necessarily produce more double-labeled cells. In fact, the lowest rate of double labeling occurred in the animal with the largest number of cells containing either BDA or DiY. We conclude that RC-multipolar cells are distinguished from radiate multipolar cells by their projection to the contralateral CN.

DISCUSSION

In the introduction, we reviewed work pertaining to the structural and functional classes of VCN multipolar cells. Two important points were that there are more physiological unit types than there are morphological classes, and that more than one unit type can be recorded from the same structural class. We are not the first to raise these points (Godfrey et al., 1975; Bourk, 1976). Rather, we raised them to highlight the gap between the physiological diversity of multipolar cells and our knowledge of the structural distinctions responsible for the different unit types. The experiments and results described here are a step toward addressing this issue.

Organizing the structural features of multipolar cells into distinct classes is challenging. Their diversity makes it difficult to distinguish between biological variability with respect to a given characteristic (e.g., dendritic morphology) and differences that are crucial for function. In addition, unlike spherical bushy cells or octopus cells that are confined to particular regions of the VCN, different types of multipolar cells appear to be broadly distributed and shuffled within the VCN. Thus, it is hard to isolate and study a particular group of multipolar neurons. Using axonal projection patterns to identify multipolar cells is a practical approach to overcoming these problems. After all, while an important goal is to define different types of multipolar cells and link them to their physiological responses to sound, an equally important goal is to know where these different messages are sent in the brain.

We used this approach to study the projections of VCN multipolar cells to the ipsilateral DCN and the contralateral CN. Our findings with respect to the source and organization of projections to each target alone are consistent with those of prior studies [ipsilateral DCN (Snyder and Leake, 1988; Oertel et al., 1990; Doucet and Ryugo, 1997; Ostapoff et al., 1999), contralateral CN (Cant and Gaston, 1982; Shore et al., 1992; Schofield and Cant, 1996a)]. New insights were revealed with a double-labeling protocol that allowed us to distinguish between cells that innervate one structure or both. Five groups of multipolar neurons were described and Table 2 displays their relationship with different structural and physiological classification schemes. Also listed are some of the known targets of each cell type at the level of the CN and the IC. New classes of multipolar cells are given names that build on those used previously to describe dendritic morphology while incorporating differences in axonal targets. For ex-

TABLE 2. Summary of multipolar cell types and axonal targets

VCN Multipolar Cells				Axonal Projections			
Structural classes			Physiological Units	Ipsilateral		Contralateral	
Doucet and Ryugo, 1997 and this study	Oertel et al., 1990	Cant, 1981	PSTH[1]	VCN	DCN	CN	IC
Planar multipolar	T-stellate	Type I	ChS, ChT	+	+	−	+
Radiate multipolar	D-stellate	Type II	OnL[2]	+	+	−	−
Radiate-commissural multipolar	D-stellate	Type II	OnC[2]	+	+	+	−
Marginal multipolar	?	?	?	?	+	−	+
Commissural multipolar	?	?	?	?	−	+	−

[1] See Table I for relevant studies
[2] One intracellularly labeled OnL unit has also been shown to project to the contralateral CN (Smith et al., 2005)

ample, RC-multipolar cells are distinguished from radiate multipolar cells by their projections to the contralateral CN. Commissural multipolar cells are separated from the other groups because they do not project to the ipsilateral DCN. Further partitioning of multipolar cells seems inevitable. For example, it is likely that subclasses of planar multipolar cells exist (Josephson and Morest, 1998), which may correspond to the ChT and ChS physiological unit types. We realize that partitioning VCN multipolar cells into different groups based on axonal projection patterns is a hypothesis to be tested. Nevertheless, this strategy facilitates synthesis with function and also helps place newly discovered types in the context of neural circuits.

Radiate and RC-Multipolar Cells

An obvious question is whether radiate and RC-multipolar cells correlate with the two major physiological units recorded from these neurons: OnC and OnL. The data germane to this question are mixed not only in terms of results, but also with respect to species and methods. For example, in guinea pigs, five intracellularly filled OnC units projected their axons to the ipsilateral DCN and the contralateral CN, whereas three OnL units only innervated the ipsilateral DCN (Arnott et al., 2004). This result suggests that RC-multipolar cells correspond to OnC units, whereas radiate multipolar cells correlate with OnL units. On the other hand, in cats, both intracellularly filled unit types were observed to project to the ipsilateral DCN and the contralateral CN (Smith et al., 2005). Furthermore, Smith et al. (2005) filled two OnC units that sent a collateral to the ipsilateral DCN but did not target cells in the contralateral CN. Finally, in rats, electrical shocks to the contralateral CN were used to evoke antidromic activity in VCN neurons (Needham and Paolini, 2003). No antidromic activity was recorded in 15 units classified as ChT or ChS, consistent with the finding that the axons of planar multipolar cells bypass the contralateral CN (Schofield and Cant, 1996b; this study). For 12 units classified as OnC, 7 were antidromically activated and 5 were not. To explain this mixed result, Needham and Paolini (2003) argue against incomplete activation of the pathway. Rather, they suggest that a subset of OnC units do not project their axons to the contralateral CN. The latter two studies in cats and rats suggest that the OnC and OnL unit types may only loosely correlate with radiate and RC-multipolar cells. Clearly, more data are needed to define how these cells respond to sound.

The neural mechanisms responsible for the OnC vs. OnL PST histogram shape are unknown. One modeling study postulated that differences in electrical characteristics were responsible for these two units (Kalluri and Delgutte, 2003a, 2003b). D-stellate (radiate and RC-multipolar) neurons, the putative neural source of the OnC and OnL unit types, appear relatively homogeneous with respect to their intrinsic mechanisms (Oertel et al., 1990; Fujino and Oertel, 2001). However, the difference in the spike generator hypothesized by Kalluri and Delgutte (2003a, 2003b) probably has not been tested. Another possibility is that different input configurations are responsible for a neuron responding as an OnC or an OnL unit. Auditory nerve fibers form synaptic terminals directly on the soma of these neurons (Cant, 1981) and this probably accounts for the large onset peak in their PST histograms (Rhode and Smith, 1986). But many of the somatic terminals appear to be inhibitory (Cant, 1981; Smith and Rhode, 1989). Inhibition can influence the shape of PST histograms in response to tones (Banks and Sachs, 1991; Blackburn and Sachs, 1992; Paolini et al., 2005), and blocking $GABA_A$ receptors while recording from PVCN onset neurons causes the post-onset firing rate to increase (Palombi and Caspary, 1992). These latter studies suggest that OnC and OnL units may differ with respect to the arrangement and/or source of inhibitory terminals on their respective cell membranes. While our data do not provide any insight into these mechanisms, they do provide a tool for isolating and studying radiate and RC-multipolar cells. Since the axonal targets of these two cell types differ, it is likely that they also differ with respect to intrinsic mechanisms and/or input configurations in ways important for their function.

CN Commissural Pathway

RC-multipolar neurons are glycinergic (Wenthold, 1987; Alibardi, 1998; Doucet et al., 1999b). Several studies have used sound or electrical shocks to activate neurons in one CN while recording from neurons in the opposite CN. Of those neurons that respond, nearly all are inhibited (Mast, 1970; Young and Brownell, 1976; Babalian et al., 2002; Shore et al., 2003; Paolini et al., 2004; Davis, 2005). Broadband sounds (e.g., white noise) are more effective inhibitors than tones (Joris and Smith, 1998; Needham and Paolini, 2003; Davis, 2005) and the inhibition is blocked with strychnine, an antagonist of glycine (Evans and Zhao, 1993; Babalian et al., 2002; Davis, 2005). In

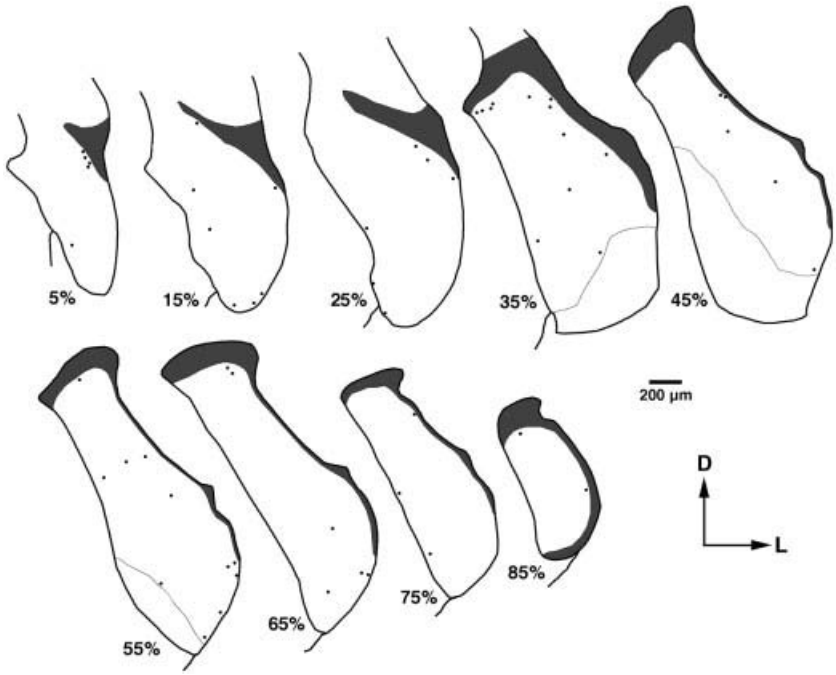

Fig. 7. Distribution of commissural multipolar neurons in one rat labeled with an FB injection in the contralateral CN. Only labeled neurons that have cell bodies less than 200 μm^2 are plotted. Each section displays the location of labeled cells combined from two adjacent sections. Percentages beneath each drawing refer to normalized distance from the posterior border of the PVCN. Very few of these neurons would be expected to project to the ipsilateral DCN (Fig. 4). Notice that these cells are scattered throughout the VCN but tend to be found near the borders of the granule cell domain (gray) and the nucleus.

contrast to the prevalence of inhibitory effects attributed to the commissural pathway, one study in rats estimated that only 40% of the VCN neurons that project to the contralateral CN are glycinergic and few, if any, are GABAergic (Alibardi, 1998). Earlier studies noted the heterogeneity of these cells with respect to size and dendritic morphology (Shore et al., 1992; Schofield and Cant, 1996a). Our data show that the neural source of the CN commissural pathway is comprised of at least two groups: (1) RC-multipolar cells and (2) commissural multipolar neurons, small- and medium-sized cells that project exclusively (in the context of this study) to the contralateral CN.

Commissural multipolar cells are interesting because all VCN multipolar neurons are thought to send a collateral axon to the ipsilateral DCN (Adams, 1983). Thus, our data suggest that these neurons represent a new type of multipolar cell. Physiological recordings from these cells are probably rare, given their small size and scarcity. In addition, commissural multipolar cells tend to be located near the margins of the CN (Fig. 7), where recordings are difficult (Ghoshal and Kim, 1997). Most are located within 50 μm of the borders of the granule cell domain, a region referred to as the small cell cap (Osen, 1969). The small cell cap contains VCN multipolar cells that appear to differ structurally (Osen, 1969; Brawer et al., 1974; Doucet and Ryugo, 1997) and functionally (Ghoshal and Kim, 1997) from those in the core of the VCN.

Commissural multipolar neurons may be excitatory since many VCN cells that project to the contralateral CN are not immunostained with antibodies against glycine or GABA (Alibardi, 1998). Activating the CN commissural pathway has been observed to increase the firing rate of some VCN and DCN neurons (Mast, 1973; Young and Brownell, 1976; Shore et al., 2003). Such excitatory effects are infrequent, but recently in guinea pigs, they were observed to increase dramatically when recordings were made from VCN neurons after raising their thresholds by plugging the ipsilateral ear (Sumner et al., 2005). Perhaps the excitatory component of the CN commissural pathway is only revealed when there is a large imbalance in the overall activity between the two cochlear nuclei. When assessing the role of RC- and commissural multipolar neurons in brain stem circuits, it is important to keep two facts in mind. Their total number is estimated to be 400–600 and thus constitute less than 4% of VCN projection neurons (Kulesza et al., 2002), and unlike the majority of VCN multipolar cells, RC- and commissural multipolar neurons do not project to the contralateral IC (Schofield and Cant, 1996b). Thus, these neurons shape neural codes in the lower brain stem rather than directly carry information about sounds to higher levels of the auditory system.

ACKNOWLEDGMENTS

The authors thank Hugh Cahill and Conor Sheehy for technical help.

LITERATURE CITED

Adams JC. 1979. Ascending projections to the inferior colliculus. J Comp Neurol 183:519–538.

Adams JC. 1983. Multipolar cells in the ventral cochlear nucleus project to the dorsal cochlear nucleus and the inferior colliculus. Neurosci Lett 37:205–208.

Adams JC. 1997. Projections from octopus cells of the posteroventral cochlear nucleus to the ventral nucleus of the lateral lemniscus in cat and human. Aud Neurosci 3:335–350.

Alibardi L. 1998. Ultrastructural and immunocytochemical characterization of commissural neurons in the ventral cochlear nucleus of the rat. Anat Anz 180:427–438.

Arnott RH, Wallace MN, Shackleton TM, Palmer AR. 2004. Onset neurones in the anteroventral cochlear nucleus project to the dorsal cochlear nucleus. J Assoc Res Otolaryngol 5:153–170.

Babalian AL, Jacomme AV, Doucet JR, Ryugo DK, Rouiller EM. 2002. Commissural glycinergic inhibition of bushy and stellate cells in the anteroventral cochlear nucleus. Neuroreport 13:555–558.

Badea TC, Nathans J. 2004. Quantitative analysis of neuronal morphologies in the mouse retina visualized by using a genetically directed reporter. J Comp Neurol 480:331–351.

Banks MI, Sachs MB. 1991. Regularity analysis in a compartmental model of chopper units in the anteroventral cochlear nucleus. J Neurophysiol 65:606–629.

Blackburn CC, Sachs MB. 1989. Classification of unit types in the anteroventral cochlear nucleus: PST histograms and regularity analysis. J Neurophysiol 62:1303–1329.

Blackburn CC, Sachs MB. 1992. Effects of off-BF tones on responses of chopper units in ventral cochlear nucleus: I, regularity and temporal adaptation patterns. J Neurophysiol 69:124–143.

Bourk TR. 1976. Electrical responses of neural units in the anteroventral cochlear nucleus of the cat. PhD dissertation. Cambridge, MA: Department of Electrical Engineering, Massachusetts Institute of Technology.

Brawer JR, Morest DK, Kane EC. 1974. The neuronal architecture of the cochlear nucleus of the cat. J Comp Neurol 155:251–300.

Cant NB. 1981. The fine structure of two types of stellate cells in the anterior division of the anteroventral cochlear nucleus of the cat. Neuroscience 6:2643–2655.

Cant NB. 1982. Indentification of cell types in the anteroventral cochlear nucleus that project to the inferior colliculus. Neurosci Lett 32:241–246.

Cant NB, Gaston KC. 1982. Pathways connecting the right and left cochlear nuclei. J Comp Neurol 212:313–326.

Cant NB, Benson CG. 2003. Parallel auditory pathways: projection patterns of the different neuronal populations in the dorsal and ventral cochlear nuclei. Brain Res Bull 60:457–474.

Carcieri SM, Jacobs AL, Nirenberg S. 2003. Classification of retinal ganglion cells: a statistical approach. J Neurophysiol 90:1704–1713.

Connaughton VP, Graham D, Nelson R. 2004. Identification and morphological classification of horizontal, bipolar, and amacrine cells within the zebrafish retina. J Comp Neurol 477:371–385.

Dacey DM, Peterson BB, Robinson FR, Gamlin PD. 2003. Fireworks in the primate retina: in vitro photodynamics reveals diverse LGN-projecting ganglion cell types. Neuron 37:15–27.

Davis KA. 2005. Contralateral effects and binaural interactions in dorsal cochlear nucleus. J Assoc Res Otolaryngol 6:280–296.

Doucet JR, Ryugo DK. 1997. Projections from the ventral cochlear nucleus to the dorsal cochlear nucleus in rats. J Comp Neurol 385:245–264.

Doucet JR, Cahill HB, Ohlrogge M, Ryugo DK. 1999a. Ventral cochlear nucleus multipolar neurons that innervate the dorsal cochlear nucleus differ in their projections outside the cochlear nucleus. St. Petersburg, FL: 22nd Annual Meeting of Association for Research in Otolaryngology.

Doucet JR, Ross AT, Gillespie MB, Ryugo DK. 1999b. Glycine immunoreactivity of multipolar neurons in the ventral cochlear nucleus which project to the dorsal cochlear nucleus. J Comp Neurol 408: 515–531.

Evans EF, Zhao W. 1993. Varieties of inhibition in the processing and control of processing in the mammalian cochlear nucleus. Prog Brain Res 97:117–126.

Ferragamo MJ, Golding NL, Oertel D. 1998. Synaptic inputs to stellate cells in the ventral cochlear nucleus. J Neurophysiol 79:51–63.

Friauf E, Ostwald J. 1988. Divergent projections of physiologically characterized rat ventral cochlear nucleus neurons as shown by intra-axonal injection of horseradish peroxidase. Exp Brain Res 73:263–284.

Friedland DR, Pongstaporn T, Doucet JR, Ryugo DK. 2003. Ultrastructural examination of the somatic innervation of ventrotubercular cells in the rat. J Comp Neurol 459:77–89.

Fujino K, Oertel D. 2001. Cholinergic modulation of stellate cells in the mammalian ventral cochlear nucleus. J Neurosci 21:7372–7383.

Ghoshal S, Kim DO. 1997. Marginal shell of the anteroventral cochlear nucleus: single-unit response properties in the unanesthetized decerebrate cat. J Neurophysiol 77:2083–2097.

Godfrey DA, Kiang NY, Norris BE. 1975. Single unit activity in the posteroventral cochlear nucleus of the cat. J Comp Neurol 162:247–268.

Harrison JM, Irving R. 1965. The anterior ventral cochlear nucleus. J Comp Neurol 124:15–42.

Harrison JM, Irving R. 1966. The organization of the posterior ventral cochlear nucleus in the rat. J Comp Neurol 126:391–401.

Joris PX, Smith PH. 1998. Temporal and binaural properties in dorsal cochlear nucleus and its output tract. J Neurosci 18:10157–10170.

Josephson EM, Morest D. 1998. A quantitative profile of the synapses on the stellate cell body and axon in the cochlear nucleus of the chinchilla. J Neurocytol 27:841–864.

Kalluri S, Delgutte B. 2003a. Mathematical models of cochlear nucleus onset neurons: I, point neuron with many weak synaptic inputs. J Comp Neurosci 14:71–90.

Kalluri S, Delgutte B. 2003b. Mathematical models of cochlear nucleus onset neurons: II, model with dynamic spike-blocking state. J Comp Neurosci 14:91–110.

Kim DO, Parham K, Sirianni JG, Chang SO. 1991. Spatial response profiles of posteroventral cochlear nucleus neurons and auditory-nerve fibers in unanesthetized decerebrate cats: response to pure tones. J Acoust Soc Am 89:2804–2817.

Kulesza RJ, Vinuela A, Saldana E, Berrebi AS. 2002. Unbiased stereological estimates of neuron number in subcortical auditory nuclei of the rat. Hear Res 168:12–24.

Lorente de Nó R. 1981. The primary acoustic nuclei. New York: Raven Press.

Mast TE. 1970. Binaural interaction and contralateral inhibition in dorsal cochlear nucleus of the chinchilla. J Neurophysiol 33:108–115.

Mast TE. 1973. Dorsal cochlear nucleus of the chinchilla: excitation by contralateral sound. Brain Res 62:61–70.

Needham K, Paolini AG. 2003. Fast inhibition underlies the transmission of auditory information between cochlear nuclei. J Neurosci 23:6357–6361.

Oertel D, Wu SH, Garb MW, Dizack C. 1990. Morphology and physiology of cells in slice preparations of the posteroventral cochlear nucleus of mice. J Comp Neurol 295:136–154.

Osen KK. 1969. Cytoarchitecture of the cochlear nuclei in the cat. J Comp Neurol 136:453–482.

Osen KK. 1970. Afferent and efferent connections of three well-defined cell types of the cat cochlear nucleus. In: Anderson P, Jansen JKS, editors. Excitatory synaptic mechanisms. Oslo: Universitetsforlaget. p 295–300.

Ostapoff EM, Morest DK, Parham K. 1999. Spatial organization of the reciprocal connections between the cat dorsal and anteroventral cochlear nuclei. Hear Res 130:75–93.

Palmer AR, Wallace MN, Arnott RH, Shackleton TM. 2003. Morphology of physiologically characterised ventral cochlear nucleus stellate cells. Exp Brain Res 153:418–426.

Palombi PS, Caspary DM. 1992. GABAA receptor antagonist bicuculline alters response properties of posteroventral cochlear nucleus neurons. J Neurophysiol 67:738–746.

Paolini AG, Clark GM. 1999. Intracellular responses of onset chopper neurons in the ventral cochlear nucleus to tones: evidence for dual-component processing. J Neurophysiolol 81:2347–2359.

Paolini AG, Clarey JC, Needham K, Clark GM. 2004. Fast inhibition alters first spike timing in auditory brainstem neurons. J Neurophysiol 92:2615–2621.

Paolini AG, Clarey JC, Needham K, Clark GM. 2005. Balanced inhibition and excitation underlies spike firing regularity in ventral cochlear nucleus chopper neurons. Eur J Neurosci 21:1236–1248.

Pfeiffer RR. 1966. Classification of response patterns of spike discharges for units in the cochlear nucleus: tone burst stimulation. Exp Brain Res 1:220–235.

Rhode WS, Oertel D, Smith PH. 1983. Physiological response properties of cells labeled intracellularly with horseradish peroxidase in cat ventral cochlear nucleus. J Comp Neurol 213:448–463.

Rhode WS, Smith PH. 1986. Encoding timing and intensity in the ventral cochlear nucleus of the cat. J Neurophysiol 56:261–286.

Rhode WS, Greenberg S. 1994. Lateral suppression and inhibition in the cochlear nucleus of the cat. J Neurophysiol 71:493–514.

Rouiller EM, Ryugo DK. 1984. Intracellular marking of physiologically characterized cells in the ventral cochlear nucleus of the cat. J Comp Neurol 225:167–186.

Rowe MH, Stone J. 1977. Naming of neurons: classification and naming of cat retinal ganglion cells, Brain Behav Evol 14:185–216.

Schofield BR. 1995. Projections from the cochlear nucleus to the superior paraolivary nucleus in guinea pigs. J Comp Neurol 360: 135–149.

Schofield BR, Cant NB. 1996a. Origins and targets of commissural connections between the cochlear nuclei in guinea pigs. J Comp Neurol 375:128–146.

Schofield BR, Cant NB. 1996b. Projections from the ventral cochlear nucleus to the inferior colliculus and the contralateral cochlear nucleus in guinea pigs. Hear Res 102:1–14.

Shore SE, Godfrey DA, Helfert RH, Altschuler RA, Bledsoe SC Jr. 1992. Connections between the cochlear nuclei in guinea pig. Hear Res 62:16–26.

Shore SE, Sumner CJ, Bledsoe SC, Lu J. 2003. Effects of contralateral sound stimulation on unit activity of ventral cochlear nucleus neurons. Exp Brain Res 153:427–435.

Smith PH, Rhode WS. 1989. Structural and functional properties distinguish two types of multipolar cells in the ventral cochlear nucleus. J Comp Neurol 282:595–616.

Smith PH, Massie A, Joris PX. 2005. Acoustic stria: anatomy of physiologically characterized cells and their axonal projection patterns. J Comp Neurol 482:349–371.

Snyder RL, Leake PA. 1988. Intrinsic connections within and between cochlear nucleus subdivisions in cat. J Comp Neurol 278:209–225.

Sumner CJ, Tucci DL, Shore SE. 2005. Responses of ventral cochlear nucleus neurons to contralateral sound after conductive hearing loss. J Neurophysiol 94:4234–4243.

Vater M, Feng AS. 1990. Functional organization of ascending and descending connections of the cochlear nucleus of horseshoe bats. J Comp Neurol 292:373–395.

Wenthold RJ. 1987. Evidence for a glycinergic pathway connecting the two cochlear nuclei: an immunocytochemical and retrograde transport study. Brain Res 415:183–187.

Winter IM, Palmer AR. 1995. Level dependence of cochlear nucleus onset unit responses and facilitation by second tones or broadband noise. J Neurophysiol 73:141–159.

Young ED, Brownell WE. 1976. Responses to tones and noise of single cells in dorsal cochlear nucleus of unanesthetized cats. J Neurophysiol 39:282–300.

Young ED, Robert J-M, Shofner WP. 1988. Regularity and latency of units in ventral cochlear nucleus: Implications for unit classification and generation of response properties. J Neurophysiol 60:1–29.

Zhang S, Oertel D. 1993. Tuberculoventral cells of the dorsal cochlear nucleus of mice: intracellular recordings in slices. J Neurophysiol 69:1409–1421.